

# How the melanin concentration in the skin affects the fluorescence-spectroscopy signal formation

V. V. Dremin<sup>1,2</sup> and A. V. Dunaev<sup>1</sup>

<sup>1</sup>State University—Academic—Scientific Manufacturing Complex, Orel, Russia

<sup>2</sup>e-mail: dremin\_viktor@mail.ru

(Received April 14, 2015)

Opticheskiĭ Zhurnal **83**, 57–64 (January 2016)

The influence of various melanin concentrations on the endogenous fluorescence intensity of biological tissue has been experimentally studied, and the fluorescence signals have been modeled by the Monte Carlo method. The modeling is based on a four-layer optical model of the skin, using known optical parameters of skin with various melanin concentrations. The fluorescence spectra obtained by the Monte Carlo method agrees with the results of the experimental investigations. © 2016 Optical Society of America.

OCIS codes: (170.6280) Spectroscopy, fluorescence and luminescence; (170.6510) Spectroscopy, tissue diagnostics.

<http://dx.doi.org/10.1364/JOT.83.000043>

## INTRODUCTION

Significant progress and achievements in photonics in recent years have resulted in explosive development of optical noninvasive diagnostics in biomedicine [1]. One such method relates to fluorescence spectroscopy (FS).

Biological tissues contain various endogenous fluorophores, such as NADH, FAD, aromatic amino acids, structural proteins, etc. The optical properties of these fluorophores are sensitive to the metabolic status of the tissue, and this makes fluorescence spectroscopy a valuable tool for investigating the state of biological tissues [2–4].

A number of processes occur in the skin before the probe radiation emerges from the tissue and reaches the detector: refraction at the boundary of the media and absorption by melanin and hemoglobin fractions, along with Mie scattering at large collagen fibers and Rayleigh scattering at smaller ones. The fluorescence of biological tissue thus strongly depends on its optical properties, and it is therefore extremely important to theoretically estimate how they affect the signal formation. Among other things, it is crucial to model the signals in FS because of the need to find a basis for the medical-technology requirements (MTRs) on FS devices [5]. Thus, the influence of tissue hyperemia on the recorded signal in optical tissue oximetry and FS was investigated earlier [6,7].

The influence of one of the tissue chromophores on the formation of the fluorescence signal was investigated for this paper. This chromophore is melanin, which is one of the most widespread natural pigments and is largely responsible for the optical properties of skin [8].

A similar question has been considered in a number of publications. Thus, an optical model of the diffuse reflection of skin was obtained in [9] in order to analyze the pigmented and depigmented sections of skin in patients with vitiligo. The influence of melanin on the transmission and reflection spectrum was considered in [10]. The reflection and fluorescence

of skin in three states (normal skin, blue vitiligo, and vitiligo) was investigated in [11,12]. However, no studies of the spectra of endogenous fluorescence on representatives with various ethnic types of skin could be found. This paper will be useful in this connection for subsequent development of a FS method, including its instrumental implementation on the basis of relevant MTRs, taking into account various melanin concentrations in the patients' skin.

## MATERIALS AND METHODS

### Experimental studies

The LAKK-M multifunctional laser noninvasive diagnostic complex (OOO Lazma Scientific Production Enterprise, Russia) was used for the experimental studies [13]. It is intended for the investigation of the state of biological tissue by simultaneously using several optical noninvasive technologies: laser Doppler flowmetry, optical tissue oximetry, pulse oximetry, and FS. Only the data of the FS channel were analyzed in this paper, with a distance of 1 mm between the probing and receiving fibers.

Experimental test studies were carried out with the participation of eight assumed healthy volunteers (including one of the authors of this article). The influence of the melanin concentration on the fluorescence spectra on various ethnic types of skin was investigated, including European (three volunteers), Indian (one), Arabic (one), and African (three). The percentage of melanin in the basal layer of the epidermis can vary from 1% to 43% in this case [14].

The measurements were made at two points of the biological tissue: on the skin of the pad of the middle finger of the right hand—a weakly pigmented region in all the volunteers—and on the skin of the forearm (at the middle of a line 3–4 cm above the styloid processes of the ulna and the radius) in a zone with pronounced differences in the melanin content relative to each skin type. The recorded parameters to be

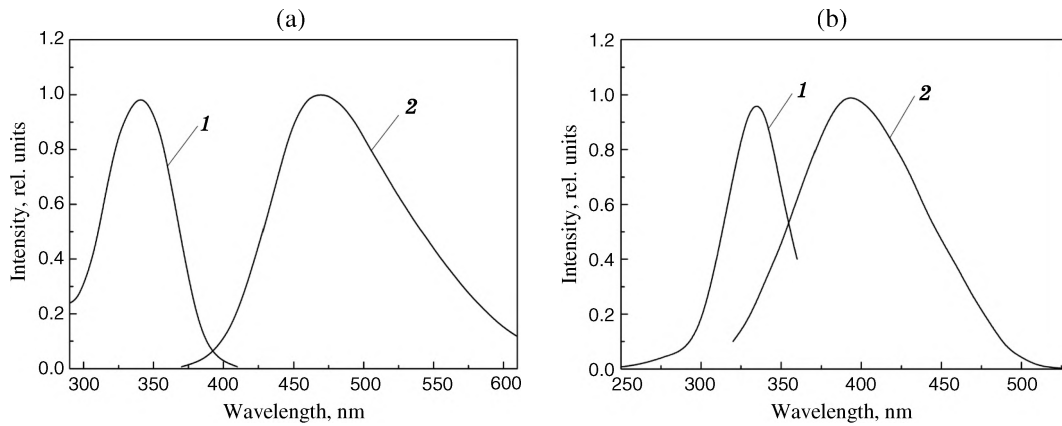


FIG. 1. Absorption (1) and fluorescence (2) spectra of (a) NADH and (b) collagen.

analyzed were the fluorescence intensities of NADH,  $I_{\text{NADH}}$  (peak in the 460–470-nm region), and FAD,  $I_{\text{FAD}}$  (about 550 nm), with excitation by UV radiation (wavelength  $\lambda = 365$  nm) and the tissue-oxygen-metabolism index, or redox reflection [15]

$$\text{RR} = I_{\text{NADH}}/I_{\text{FAD}}. \quad (1)$$

The parameters are then averaged, and the mean  $M_n$  and rms deviation  $\sigma$  are computed.

### Modeling

To describe and predict how melanin affects the fluorescence signal, a model of light propagation in biological tissue was proposed.

As a whole, the fluorescence intensity of skin is determined by the fluorescence of NADH in the epidermis and the fluorescence of collagen in the dermis [8]. NADH possesses characteristic absorption spectra, including two bands in the UV region ( $\lambda = 260$  and  $\lambda = 340$  nm), as well as a typical intrinsic fluorescence spectrum with a maximum in the interval from 460 to 480 nm [2,8,16]. In [17], the highest values of the radiation intensity of collagen were excited and recorded, respectively, at 280 and 310 nm, 265 and 385 nm, 330 and 390 nm, and 450 and 530 nm. The absorption and fluorescence spectra of NADH and collagen at an excitation wavelength of 365 nm are shown in Fig. 1.

The simultaneous presence of several fluorophores in the tissues results in a complicated total fluorescence spectrum recorded from these substances, with a different number of maxima and minima [18]. It is proposed in the model to take into account the fluorescence signals from the main fluorophores of the tissue—NADH and collagen—where, as can be seen from Fig. 1, part of the collagen spectrum overlaps the NADH spectrum. As a result, the total signal will be recorded in the 400–550-nm range analyzed here. The form of the total spectrum can vary, depending on the fluorescence intensity of each of the fluorophores under consideration.

The hyperemia of the dermis in the modeling was calculated at a constant mean level of 0.2% [19].

As is well known, skin has a very complex structure, and therefore, a simplified four-layer optical model of the skin was

constructed for theoretical modeling. Incident radiation transmitted through the epidermis is absorbed to a greater extent by the melanin and excites fluorescence in the NADH. The transmitted part is incident on the dermis, where it is absorbed predominantly by the hemoglobin fractions and excites the collagen fluorescence. The remaining probe radiation and the secondary fluorescence radiation are diffusely reflected from the collagen fibers and again pass through the layers of skin, being absorbed by the hemoglobin and melanin.

The main parameters that determine the optical properties of the biological tissues and the bonds between them [14] are given in Fig. 2.

The indicated transport parameters were calculated on the basis of the data given in [14]. The parameters of the model are shown in Table 1.

The numerical modeling was carried out by the Monte Carlo method. This is currently one of the most frequently used methods of describing light propagation in biological tissues [20,21]. Its principal idea is to take absorption and scattering into account on the entire optical path of a photon through a nontransparent medium. The new possibilities of the TracePro software medium (Lambda Research Corp.), intended for analyzing light propagation in optomechanical systems, were used as a modeling tool.

Based on the given parameters, the absorption in the biological tissue is taken into account by the Bouguer–Lambert–Beer law,

$$\Phi = \Phi_0 \exp(-\mu_a t), \quad (2)$$

|                     |                         |                    |
|---------------------|-------------------------|--------------------|
| Absorption          | $\mu_a$                 | $[\text{mm}^{-1}]$ |
| Scattering          | $\mu_s$                 | $[\text{mm}^{-1}]$ |
| Scattering function | $p(\theta)$             | $[\text{sr}^{-1}]$ |
| Anisotropy factor   | $g$                     | $[-]$              |
| Refractive index    | $n$                     | $[-]$              |
| Reduced scattering  | $\mu'_s = \mu_s(1 - g)$ | $[\text{mm}^{-1}]$ |

FIG. 2. Main optical parameters of biological tissues.

TABLE 1. Four-Layer Model of Skin<sup>a</sup>

| Layer            | Thickness, $\mu\text{m}$ | Refractive index | $\mu_a$ , $\text{cm}^{-1}$ | $\mu_s$ , $\text{cm}^{-1}$ | $g$  |
|------------------|--------------------------|------------------|----------------------------|----------------------------|------|
| Horny layer      | 10                       | 1.55             | 300                        | 2200                       | 0.9  |
| Epidermis        | 100                      | 1.4              | 24.2                       | 1000                       | 0.72 |
| Papillary dermis | 200                      | 1.37             | 4.7                        | 460                        | 0.73 |
| Reticular dermis | 1000                     | 1.4              | 4.7                        | 460                        | 0.74 |

<sup>a</sup>Radiation-propagation parameters ( $\mu_a$ ,  $\mu_s$ ,  $g$ ) are given only at a wavelength of 365 nm. The optical parameters for other wavelengths are not included here but were obtained analogously, using public data.

where  $\Phi$  and  $\Phi_0$  are the transmitted and incident fluxes,  $\mu_a$  is the absorption coefficient, and  $t$  is the sample thickness.

Fresnel’s law is used to take into account the refraction or reflection at the interface of two media.

The Henyey–Greenstein function is most often chosen as the phase scattering function,

$$\text{SDF} = p(\theta) = \frac{1 - g^2}{4\pi(1 + g^2 - 2g \cos \theta)}, \quad (3)$$

where  $g$  is the anisotropy factor. Parameter  $g$  can take values from  $-1$  to  $1$ . The rays are predominantly scattered in the forward direction when  $g > 0$  and in the reverse direction when  $g < 0$ . If  $g = 0$ , the scattering is isotropic—i.e., it is identical in all directions.

When a ray passes through a scattering medium, it propagates to a random distance  $x$ , governed by the probability distribution

$$P(x)dx = \exp(-\mu_s x)dx, \quad (4)$$

where  $\mu_s$  is the scattering coefficient.

When a ray interacts with a material that is thin by comparison with the free path length, it passes through the material without scattering. Conversely, if the material is thick, the ray will be scattered with high probability.

The fluorescence is modeled in TracePro, taking into account the fluorescence properties in combination with the properties of the material of the object and using the laws given above. The specified parameters include the relative absorption  $ab(\lambda)$  and the relative excitation  $ex(\lambda)$ , normalized to the molar extinction coefficient  $K_{\text{peak}}$  and the relative emission  $em(\lambda)$ . The concentration of fluorescent substance is established by introducing the molar concentration  $C_{\text{molar}}$ .

The absorption coefficient of fluorophores is defined in a medium as

$$\mu_a(\lambda) = ab(\lambda)K_{\text{peak}}C_{\text{molar}}, \quad (5)$$

and the path length before absorption is

$$d(\lambda) = -\log(x)/\mu_a(\lambda), \quad (6)$$

where  $x$  is a random number from 0 to 1.

The ratio of the number of photons that participate in the process to the number of photons that have been absorbed by the system is determined by specifying the quantum efficiency QE in the medium.

## RESULTS AND DISCUSSION

### Experimental Studies

The fluorescence intensity in the region of the forearm decreases as the skin pigment increases, and the statistical differences were confirmed using the Mann–Whitney U-criterion (Fig. 3 and Table 2). No fluorescence signal was actually recorded in volunteer D.

Data obtained in a separate, supplementary investigation in the same regions of the skin of a dark-skinned woman 25 years old show that fluorescence is also absent when excitation is produced by light with  $\lambda = 365$  and  $532$  nm. When the excitation is produced by radiation with  $\lambda = 635$  nm, the fluorescence was stronger than in the first two cases of excitation. This indicates that it is expedient to use this method to determine fluorophores that can be excited and fluoresce in the spectral region starting in the near-IR region, as well as that the melanin fluorescence can be directly recorded. In confirmation of this assumption, the latter results of multiphoton spectroscopy (780–820 nm) displayed substantial differences in the fluorescence of eu- and pheomelanin in normal tissues and in developed melanoma [22].

The scatter of the results of the measurements (including those in [7,23]) indicates that it is necessary to create an adequate mathematical model to describe the properties of biological tissue, especially of the fluorescence.

### Modeling

An image of the propagation of fluorescent rays inside tissue, obtained by means of TracePro with the filtered excitation wavelength (365 nm), is shown in Fig. 4.

A family of model spectra as the melanin concentration varied in the range 1%–43% [Fig. 5(a)] was obtained from the results of the modeling. As can be seen, the melanin fluorescence signal is virtually absent beyond a concentration of 15%.

It should be pointed out that the presented model spectra are somewhat different from those obtained experimentally for the total spectra of the various components [Fig. 5(b)]. The more intense experimental signal in the 500–570-nm wavelength region can be caused by the fact that other fluorophores (FAD, pyridoxine, etc.) that are neglected in the modeling can contribute to the total fluorescence spectrum of the skin under actual conditions. Other chromophores (bilirubin, porphyrins, carotenoids, etc.) that are not included in the modeling also affect the shape of the actual experimental spectrum in the 400–480-nm range, and this causes the model and experimental spectra to differ [24].

One problem of the FS method is allowing for the intensity loss of the exciting radiation. This makes it hard in the long run to calibrate the given type of diagnostic devices—namely, to establish how the values of a measured quantity depend on the indices of a device. Thus, the influence of melanin should be taken into account both in the calibration of the

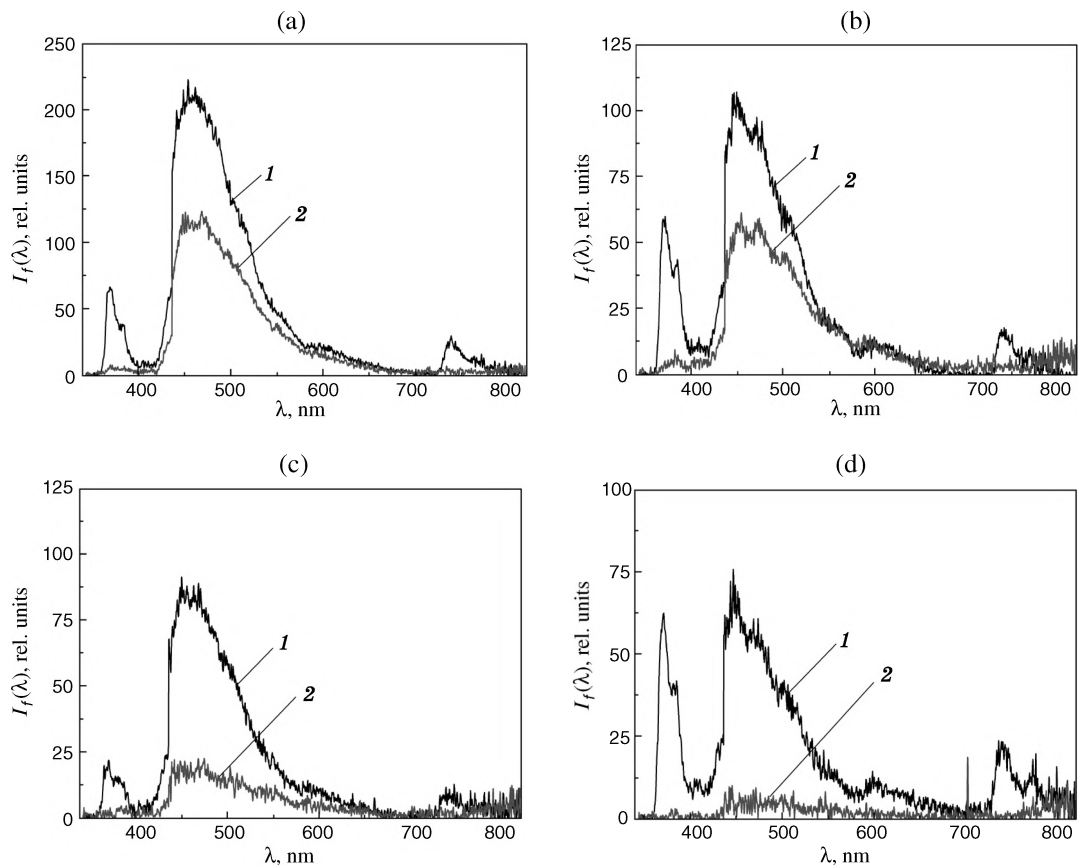


FIG. 3. Examples of the fluorescence spectra of the skin of various ethnic types on the surface of the finger (1) and forearm (2). See text for explanation.

TABLE 2. Results of Experimental Studies

| $\lambda$ , nm | Ethnic skin type       | $M_k \pm \sigma$ , rel. units |                 |               |                  |                 |               |
|----------------|------------------------|-------------------------------|-----------------|---------------|------------------|-----------------|---------------|
|                |                        | Surface of finger             |                 |               | Forearm          |                 |               |
|                |                        | NADH                          | FAD             | RR            | NADH             | FAD             | RR            |
| 365            | European (A), $n = 50$ | $220.2 \pm 48.9$              | $49.2 \pm 11.8$ | $4.4 \pm 0.5$ | $120.1 \pm 11.8$ | $21.3 \pm 3.3$  | $5.6 \pm 0.6$ |
|                | Indian (B), $n = 27$   | $110.1 \pm 22.3$              | $25.2 \pm 6.6$  | $4.9 \pm 0.7$ | $60.9 \pm 14.2$  | $15.4 \pm 5.1$  | $4.0 \pm 0.5$ |
|                | Arabic (C), $n = 13$   | $84.3 \pm 37.7$               | $25.5 \pm 12.6$ | $3.3 \pm 0.3$ | $25.9 \pm 3.9$   | $8.9 \pm 2.5$   | $2.9 \pm 0.4$ |
|                | African (D), $n = 3$   | $75.4 \pm 30.5$               | $22.3 \pm 17.5$ | $3.4 \pm 0.4$ | $\rightarrow 0$  | $\rightarrow 0$ | –             |

means of recording the fluorescence signal and in providing a basis of MTRs for the FS devices.

These results need to be taken into account when planning electronic modules of the device. Thus, for example, it is necessary to impose special requirements on the choice of the photodetector (PD), since it needs to have high photometric accuracy.

Thus, PDs based on the TCD1304AP and ILX511 CCDs, which are widely used in modern spectroscopy, were considered for this project, and their noise characteristics (the SNRs) were evaluated, taking into account the results of our modeling. The goal of the calculation is to determine the threshold (minimum) radiation flux incident on the PD at which the useful signal level equals the dark noise of the CCD, since it is assumed that it makes the dominant contribution to the overall

noise of the PD. Our calculations showed that, for a low melanin concentration in the skin (at the 1% level) and an accumulation time of 10 ms, the SNR will be 60–70 dB. As the pigmentation increases, the SNR decreases and equals 0–5 dB at a concentration of 11%–12%, and this makes it difficult to distinguish the useful low-intensity fluorescence signal on a noisy background. In absolute photometric quantities, this corresponds to a radiation flux of  $2.92 \times 10^{-15}$  W for the TCD1304AP and  $6.15 \times 10^{-15}$  W for the ILX511. The linear ILX511 CCD, despite higher sensitivity on the whole, possesses a lower SNR, as illustrated in Fig. 6.

Our results thus confirm that it is necessary to find a basis for the MTRs when the optoelectronic modules of devices are being designed both for FS and for noninvasive diagnosis in medicine as a whole.

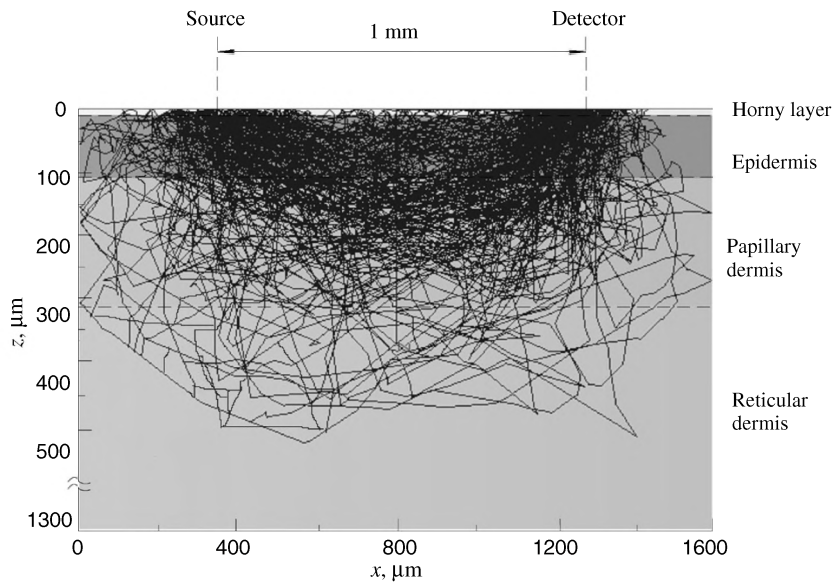


FIG. 4. Propagation of fluorescent rays inside tissue.

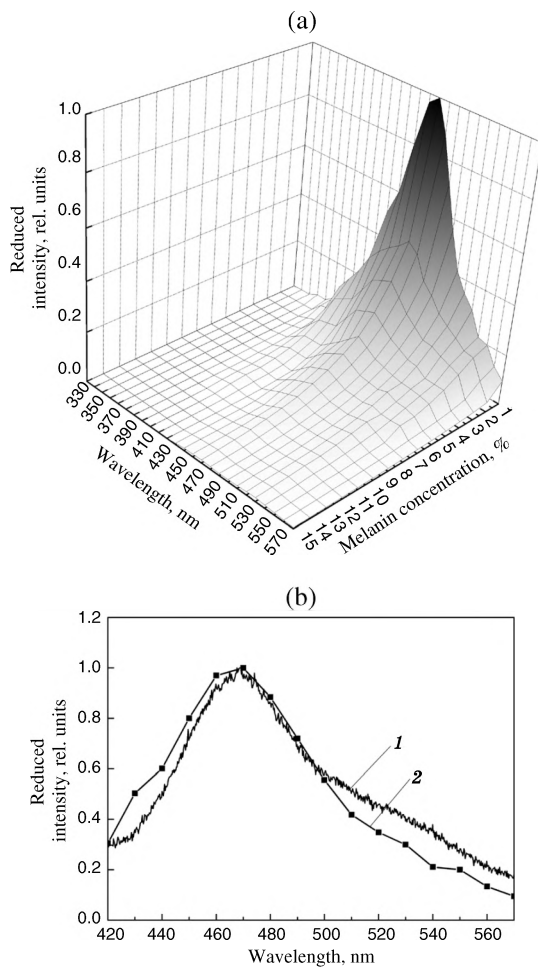


FIG. 5. (a) Family of model spectra calculated by the Monte Carlo method and (b) comparison of experimental (1) and model (2) spectra in the case of European-type skin with 1% melanin concentration.

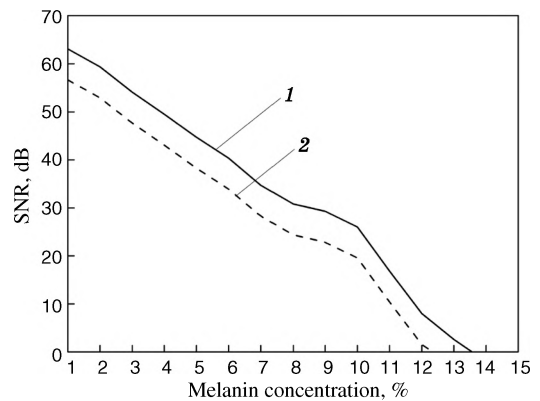


FIG. 6. Dependences of the SNR on the melanin concentration for CCDs TCD1304AP (1) and ILX511 (2).

## CONCLUSION

The influence of the concentration of skin melanin on the intensity of the recorded fluorescence spectra has been estimated, and it has been shown that the current approach to recording the fluorescence spectra in representatives of various ethnic groups is limited. Based on the optical model of the skin developed here and using the Monte Carlo method for modeling, it is possible to analyze radiation propagation in biological tissue as a whole. This can be useful in other noninvasive optical research methods.

One direction of development of representative modeling is the possibility of using spectrophotometric methods to determine the optical properties of intact (healthy) tissues and tissues damaged by various destructive processes, after which these data are used when constructing a model. It is thus possible to obtain *a priori* information for subsequent qualitative

differentiation of healthy and damaged tissues in actual clinical studies.

## ACKNOWLEDGMENT

This work was carried out as a basic part of a state program of the RF Ministry of Education and Science for the Federal State Budgetary Educational Institute of Higher Professional Education State University—Academic—Scientific Manufacturing Complex (No. 310).

1. V. V. Tuchin, ed., *Handbook of Optical Biomedical Diagnostics* (SPIE, Bellingham, Wash., 2002; Fizmatlit, Moscow, 2007), vol. 1.
2. J. R. Lakowicz, *Principles of Fluorescence Spectroscopy* (Plenum Press, New York, 1983; Mir, Moscow, 1986).
3. N. Akbar, S. G. Sokolovski, A. V. Dunaev, J. J. Belch, E. U. Rafailov, and F. Khan, "In vivo noninvasive measurement of skin autofluorescence biomarkers relate to cardiovascular disease in mice," *J. Microsc.* **255**(1), 42–48 (2014).
4. O. D. Smirnova, D. A. Rogatkin, and K. S. Litvinova, "Collagen as in vivo quantitative fluorescent biomarkers of abnormal tissue changes," *J. Innovative Opt. Health Sci.* **5**(2), 1250010 (2012).
5. D. A. Rogatkin and O. D. Smirnova, "Mathematical modelling of signals recorded in noninvasive medical laser fluorescence diagnosis," *J. Opt. Technol.* **80**(9), 566–570 (2013) [*Opt. Zh.* **80**(9), 54–60 (2013)].
6. A. V. Dunaev, E. A. Zherebtsov, D. A. Rogatkin, N. A. Stewart, S. G. Sokolovski, and E. U. Rafailov, "Substantiation of medical and technical requirements for non-invasive spectrophotometric diagnostic devices," *J. Biomed. Opt.* **18**(10), 107009 (2013).
7. A. V. Dunaev, V. V. Dremin, E. A. Zherebtsov, I. E. Rafailov, K. S. Litvinova, S. G. Palmer, N. A. Stewart, S. G. Sokolovski, and E. U. Rafailov, "Individual variability analysis of fluorescence parameters measured in skin with different levels of nutritive blood flow," *Med. Eng. Phys.* **37**(6), 574–583 (2015).
8. V. V. Tuchin, ed., *Handbook of Optical Biomedical Diagnostics* (SPIE Press, Bellingham, Wash., 2002; Fizmatlit, Moscow, 2007).
9. N. Kollias and A. Baqer, "Spectroscopic characteristics of human melanin in vivo," *J. Invest. Dermatol.* **85**(1), 38–42 (1985).
10. G. I. Petrov, A. Doronin, H. T. Whelan, I. V. Meglinski, and V. V. Yakovlev, "Human tissue color as viewed in high dynamic range optical spectral transmission measurements," *Biomed. Opt. Express* **3**(9), 2154–2161 (2012).
11. I. Hamzavi, N. Shiff, M. Martinka, Z. Huang, D. I. McLean, H. Zeng, and H. Lui, "Spectroscopic assessment of dermal melanin using blue vitiligo as an in vivo model," *Photodermatol. Photoimmunol. Photomed.* **22**(1), 46–51 (2006).
12. R. Chen, Z. Huang, H. Lui, I. Hamzavi, D. I. McLean, S. Xie, and H. Zeng, "Monte Carlo simulation of cutaneous reflectance and fluorescence measurements—the effect of melanin contents and localization," *J. Photochem. Photobiol. B* **86**(3), 219 (2007).
13. D. A. Rogatkin, S. G. Sokolovski, K. A. Fedorova, V. V. Sidorov, N. A. Stewart, and E. U. Rafailov, "Basic principles of design and functioning of multifunctional laser diagnostic system for non-invasive medical spectrophotometry," *Proc. SPIE* **7890**, 78901H (2011).
14. S. L. Jacques, "Optical properties of biological tissues: a review," *Phys. Med. Biol.* **58**(11), R37–R61 (2013).
15. B. Chance, B. Schoener, R. Oshino, F. Itshak, and Y. Nakase, "Oxidation–reduction ratio studies of mitochondria in freeze-trapped samples. NADH and flavoprotein fluorescence signals," *J. Biol. Chem.* **254**(11), 4764–4771 (1979).
16. G. A. Wagnieres, W. M. Star, and B. C. Wilson, "In vivo fluorescence spectroscopy and imaging for oncological applications," *J. Photochem. Photobiol.* **68**(5), 603–632 (1998).
17. R. Richards-Kortum, R. P. Rava, J. Baraga, M. Fitzmaurice, J. Kramer, and M. Feld, *Optronic Techniques in Diagnostic and Therapeutic Medicine* (Plenum, New York, 1990), pp. 129–138.
18. D. A. Rogatkin, "Physical principles of laser clinical fluorescence spectroscopy in vivo. Lecture," *Medit. Fiz.* (4), 78–96. (2014).
19. S. L. Jacques, "Origins of tissue optical properties in the UVA, visible, and NIR regions," *Adv. Opt. Imaging Photon Migr.* **2**, 364–369 (1996).
20. D. Y. Churmakov, I. V. Meglinski, S. A. Piletsky, and D. A. Greenhalgh, "Analysis of skin tissues spatial fluorescence distribution by the Monte Carlo simulation," *J. Phys. D* **36**(14), 1722–1728 (2003).
21. S. L. Jacques and L. Wang, "Monte Carlo modeling of light transport in tissues," *Opt.-Therm. Response Laser-Irradiat. Tissue* **12**, 73–100 (1995).
22. J. L. Silveira, F. L. Silveira, B. Bodanese, R. A. Zangaro, and M. T. T. Pacheco, "Discriminating model for diagnosis of basal cell carcinoma and melanoma in vitro based on the Raman spectra of selected biochemical," *J. Biomed. Opt.* **17**(7), 077003 (2012).
23. A. V. Dunaev, V. V. Dremin, E. A. Zherebtsov, S. G. Palmer, S. G. Sokolovski, and E. U. Rafailov, "Analysis of individual variability of the parameters in laser fluorescence diagnosis," *Biotekhnosfera* **26**(2), 39–47 (2013).
24. R. R. Anderson, "In vivo fluorescence of human skin [letter, comment]," *Arch. Dermatol.* **125**, 999–1000 (1989).